Simulation of process-dependent properties with *MAT_254 demonstrated for the 'bake-hardening' of an aluminum 6xxx alloy

Mathias Merten[1], Thomas Klöppel[1], Sebastijan Jurendic[2], Zeqin Liang[3]

[1]DYNAmore GmbH
[2]Novelis Germany GmbH
[3]Novelis Switzerland SA

1 Process-dependent Properties in LS-DYNA

Taking into account the strain and thickness distributions of cold formed parts is well established in LS-DYNA. Additionally, ***MAT_TAILORED_PROPERTIES** offers the possibility to use a tabulated set of flow curves dependent on a history variable. The physical quantity represented by the chosen history variable can be defined by the user. Getting the distribution of this history variable may be a difficult task. For press-hardening simulation exclusively, LS-DYNA offers ***MAT_244/248** to calculate the distribution of mechanical properties based on the distribution of metallurgical phases. The phase distribution is a result of the thermo-mechanically coupled simulation of the production process. To overcome the limitations of these two material models, ***MAT_GENERALIZED_PHASECHANGE** was implemented. This material has been used successfully for the simulation of press-hardening, welding and 3D-Printing. The current work presents a new field of application for ***MAT_GENERALIZED_PHASECHANGE**, simulating the “bake-hardening”-effect of specific aluminium alloys. The local final strength of hardenable aluminum alloys for automotive applications depends on the local pre-strain from the forming process and the local time-temperature-profile during paint bake. An initial approach to model this behavior is given. Implemented extensions to ***MAT_GENERALIZED_PHASECHANGE**, which enable are more precise description of the underlining mechanisms, will be shown.

2 Short overview of *MAT_254

Figure (1) shows the keyword input for ***MAT_GENERALIZED_PHASE_CHANGE/*MAT_254**. The model has been introduced in [1] and is tailored for simulating microstructure evolution in metals and the resulting properties. The parameters used for the approach presented in section (4) are coded in green.

Card 1	MID	RO	N	E	PR	MIX	MIXR	
Card 2	TASTAR	TAEND	CTE				DTEMP	
Card 3	PTLAW	PTSTR	PTEND	PTX1	PTX2	PTX3	PTX4	PTX5
Card 4	PTTAB1	PTTAB2	PTTAB3	PTTAB4	PTTAB5			
Card 5	PTEPS	PTRIP	PTLAT		NUSHIS	GRAIN	T1PHAS	T2PHAS
Card 6	SIGY1	SIGY2	SIGY3	SIGY4	SIGY5	SIGY6	SIGY7	SIGY8

Fig.1: Required cards for Mat_254 and used non-default entries (in green) for the presented approach.

Beside the standard input quantities for a LS-DYNA material in the first card, there is an additional parameter **N** for the number of phases to be taken into account. Up to 24 phases are currently supported. The sum of all phase concentrations x_i is always equal to one. The parameter **MIX** specifies the initial mixture of the phases. The elemental mixture can also be read in from a DYNAIN-file. Per default the mixture rule, **MIXR**, for all mechanical properties is a linear combination:

$$P_{total} = \sum_{i=1}^{N} x_i P_i \tag{1}$$

where P is a mechanical property and x_i denotes the concentration of phase *i*.

The parameters of the second card control the annealing algorithm, account for the thermal expansion and define a form of internal sub-cycling to resolve non-linear effects. As none of these methods are used in this contribution, the parameters are not discussed here in detail.

The third and fourth cards specify the phase transformation models between the phases. The parameter **N** influences the shape of the data referred to by the parameters in Card 3 and 4 as it determines the input structure to be a **N** by **N**-matrix, which is read by the material model as “from phase … to phase …” as is shown in figure (2).

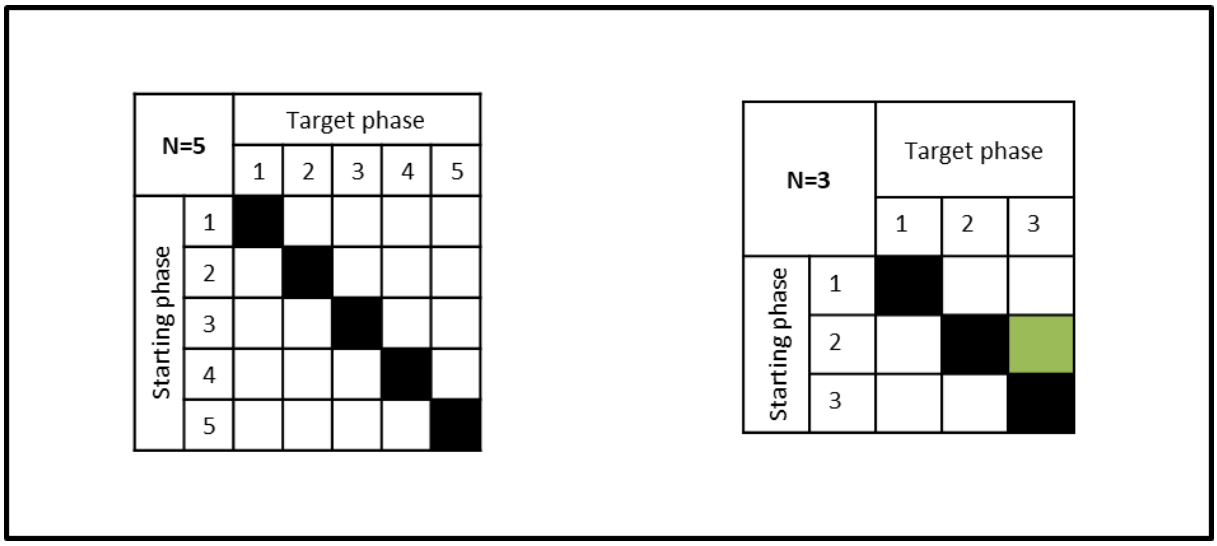

Fig.2: The number of phases to be taken into account, N, influences the shape of many other parameters. Left: Five phases considered. Right: Phase patchwork scheme for the approach used later with three phases and one transformation from phase 2 to phase 3. For that example, all matrix-like-entered parameters should look like this.

The parameter **PTLAW** on the third card is a matrix as shown in figure (2) and contains the information, between which of the **N** phases a transformation can occur. The input parameter itself refers to a 2D-table, where the abscissae are the “Starting phase”-entries and the ordinates are load curves. The abscissae of every referenced load curve represent the “Target phases”. The ordinate of every load curve determines the kinetic law for the transformation. A blank entry means no transformation.
A negative value for the load curve ordinate indicates a transformation model to be used in a heating phase, i.e. LS-DYNA will calculate a transformation rate during a time step with a temperature increase. A positive value defines a phase transition in cooling. The absolute value specifies the law of the transformation kinetic. Four kinetic laws can currently be used: values of 1, 3 and 4 are associated with press-hardening of boron steel and the second model is the generalized JMAK, shown in the integral form in equation (2).

$$x_b = x_{eq}(T)\left(x_a^0 + x_b^0\right)\left(1 - e^{-\left(\frac{t}{\tau(T)}\right)^{n(T)}}\right) \tag{2}$$

It is also possible to use the generalized JMAK independent of the temperature rate, i.e. for heating, cooling and in case of constant temperatures. For that purpose, the option “12” is available.

The parameters **PTSTR** and **PTEND** are the starting and ending temperatures of a certain transformation and thus, also pointing to scalar input values given in the matrix-like structure shown in figure (2). For temperatures outside the temperature window defined by **PTSTR** and **PTEND** LS-DYNA does not consider the corresponding transformation. The other parameters in Card 3 **PTX1** to **PTX5** are defining matrix-like data and represent the scalar parameters for the transformation laws, if there are any. The meaning of the data depends on the chosen evolution equations for the transformation.

The fourth card contains the parameters of the kinetic laws that are functions of some other variable, in most cases as function of temperature. Therefore, the matrix entries for the tables shown in figure (2), are load curve IDs and those load curves define the respective relation. Technically, LS-DYNA expects the input as 3D-tables. As stated above, the interpretation of the data varies between the different transformation laws. Here, only the input for the JMAK-like kinetic, equation (2), are discussed in detail, as the approach in section 4 is JMAK-like.

The integral form in (2) can be read as the amount of phase b after an isothermal heat treatment at temperature T and for a period of time t, i.e. $x_b = x_b(T,t)$. Phase b is formed from phase a and its concentration develops towards an equilibrium concentration, which depends on the temperature T and the initial concentrations x_a^0 and x_b^0 of phase a and b, respectively, at the beginning of the transformation. Mathematically, the equilibrium concentration is given as $x_{eq}(T)(x_a^0 + x_b^0)$, where the factor $x_{eq}(T)$ is a user-input defined in parameter **PTTAB2.** In case that there are only the two phases a and b, the sum of $(x_a + x_b)$ is always equal to one and $x_{eq}(T)$ is then the concentration of phase b for infinitely long holding times at temperature T.

The parameter $\tau(T)$ represents the relaxation time of the transformation from phase a to phase b and quantifies how fast a transformation proceeds. The classical approach is to use an Arrhenius-like grow constant. The temperature dependent relaxation time is a more general notion and it can easily be used to incorporate the classical approach by using the relation:

$$\frac{1}{\tau(T)} = k_0 e^{-\frac{Q}{RT}}. \tag{3}$$

In Arrhenius equation (3) constant k_0 is usually interpreted as jump frequency, Q as the activation energy, R the universal gas constant and T the absolute temperature.

Parameter $n(T)$ of the JMAK equation (2) is the grow-exponent and defined in **PTTAB1**, the equilibrium concentration $x_{eq}(T)$ in **PTTAB2**, and the relaxation time $\tau(T)$ in **PTTAB3**. Temperature rate effects can be taken into account by a correction function given in **PTTAB4** and **PTTAB5** that are per default equal to one.

Card 5 offers the possibility to include transformation induced strains and latent heat. In addition the user is free to specify user dependent history variables for post-processing. For that purpose, arbitrary algebraic expressions can be implemented by the user employing the keyword ***DEFINE_FUNCTION.**

The sixth card is repeated for every eight phases and contains the yield curves for every phase. Load curves, 2D- and 3D-tables are supported and enable to take temperature- and strain-rate-effects into account.

3 Short overview of strengthening mechanisms in hardenable aluminum alloys

The total strength of a 6xxx aluminum alloy is a combination of the strength of several mechanisms. According to Deschamps et al [2], the strength can be described as a sum:

$$\sigma_{total} = \sigma_{Al} + \sigma_{gb} + M(\tau_d + \tau_{ss}) + \sigma_{ppt} \tag{4}$$

were σ_{Al} is the strength of the aluminum matrix, σ_{gb} is the strengthening contribution of the grain boundaries, M the taylor factor, τ_d the contribution of stored dislocations, τ_{ss} the contribution of the

dissolved elements in solid solution, and σ_{ppt} the combined contribution of precipitates. The precipitates could be divided further into several sub-classes, like precipitation in the matrix, on the grain boundaries or along the dislocations and it is obvious that the dislocation density influences the allocation of these precipitations.

To use the precipitation-associated strengthening mechanisms, the material needs to be in a state of supersaturated solid solution, which can be achieved by holding it above a certain temperature for a specified duration, followed by a quench to avoid the formation of other phases. It is in that state, in which the material is usually formed. In figure (3), an overview of the process chain is outlined.

After forming, the single parts are joined to the automotive car structure and the structure is painted. After painting the body in white undergoes a paint curing, or paint bake, process. The heat input during paint bake activates the formation of precipitation from the supersaturated solid solution. The time-temperature-history mainly influences the process speed of precipitation and yields different allocations of the different precipitation in the final part and thus, a scatter in the mechanical properties.

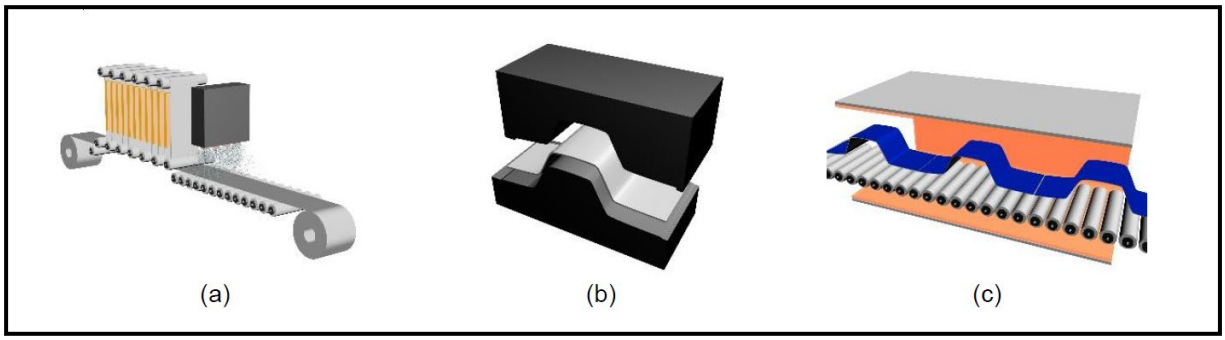

Fig.3: Process chain for automotive aluminum alloys: final annealing with heating and rapid cooling (a), forming (b) and paint bake (c) [3]

4 Approach for an Aluminum Alloy

Figure (4) shows the contribution of several mechanisms to the final yield strength of an EN AW 6xxx alloy depending on the duration of a heat treatment at 185°C according to [3]. The effect of different precipitation mechanisms (nucleation and grow at different type of sites) is summed up to one combined contribution (called “Precipitates”).

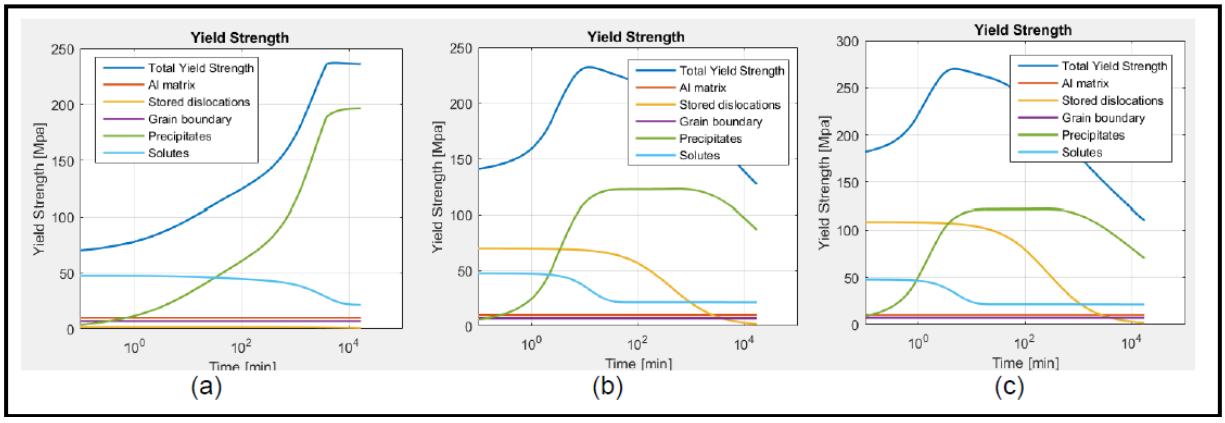

Fig.4: Contribution of several mechanisms to final Yield Strength of an EN AW 6xxx alloy as a function of holding time at 185°C. With no pre-strain (a), with 5% (b) and 10% pre-strain (c) [3]

The curves in figure 4 (a) allow extracting the following approach:

$$\sigma_{Y\ total}(T,t) = \sigma_{Y\ constants} + \sigma_{Y\ increasing}(T,t) + \sigma_{Y\ decreasing}(T,t), \quad (5)$$

where $\sigma_{Y\ constants}$ represents the sum of “Al matrix”, “Grain boundary” and “Stored dislocations”, i.e. the contribution to the yield strength that do not depend on temperature or holding time. The second term

$\sigma_{Y\ increasing}$ of (5) is identical to the contribution of the precipitates (or precipitations) and, finally, the contribution $\sigma_{Y\ decreasing}$ is associated with the contribution of the solutes.

Comparing equation (5) with equation (1) offers the possibility to interpret the precipitation mechanism as a phase transformation in the manner of ***MAT_254** with **N** set to three. Under the assumption that the contribution of a mechanism is a product of a constant strength and a variable concentration, the necessary parameters for a kinetic law like JMAK can be extracted. As only information for the product of strength and concentration is available, there are an infinite number of possible combinations of mechanism-associated phases and their respective strength.

Table (1) contains one of the possible combinations extracted from figure (4). It can be stated, that the concentration of the solutes-associated phase at the end is ~55% of its starting concentration. It is further assumed that the remaining ~45% are forming the precipitation-associated phase. Consequently, the reduction by 25 MPa due to the decreasing solute-associated phase leads to an increase by 185 MPa resulting from the precipitation-associated phase formation.

Time	10e-1	10e4
Contribution of Solutes to Yield Strength	47 MPa	22 MPa
% of starting	100%	55%

Table 1: Extracted data for solutes

In the proposed approach, it is impossible to uniquely derive the starting concentration of all three phases, but the choice of the starting concentration determines the *Strength Factor* of every phase. Table (2) contains a possible combination of initial concentrations and *Strength Factors*. Naturally, as there is no initial precipitates, the *Strength Factor* of the precipitates-associated phase is still unknown.

	Concentration	Contribution	*Strength Factor*
Constant-associated phase	0.4	30 MPa	75 MPa
Solutes-associated phase	0.6	47 MPa	78 MPa
Precipitates-associated phase	0.0	0 MPa	
Sum	1.0	87 MPa	-

Table 2: One possible combination of initial (t=1e-1min) concentrations and the corresponding Strength Factor.

All the assumed states so far allow writing down a similar table for the end of the time scale in figure (2). The result of this process is shown in table (3). As the *Strength Factor* should remain constant, the *Strength Factor* of the precipitate-associated phase can easily been calculated. By defining a transformation, for which the precipitation-associated phase can reach a volume fraction of 1, the final yield strength would be 685 MPa. Based on our definitions, this cannot be reached, because a maximum of 45% of the starting concentration of the solute-associated phase can transform into the precipitate-associated phase.

	Concentration	Contribution	*Strength Factor*
Constant-associated phase	0.4	30 MPa	75 MPa
Solutes-associated phase	0.6 * 0.55 = 0.33	22 MPa	78 MPa
Precipitates-associated phase	0.6 * 0.45 = 0.27	185 MPa	685 MPa
Sum	1.0	237 MPa	-

Table 3: Corresponding concentrations and the corresponding Strength Factor at the end (t=10e4 minutes).

From the reduction of the yield strength contribution of the solute-associated phase with increasing holding times, the kinetic parameters for the JMAK equation (namely $X_{precipitation\ eq}$, τ and n) can be calculated for a given temperature. There are different fitting procedures available to determine these parameters. Only if the JMAK evolution equation describes the physical process perfectly, the different fitting approaches will result in the same set of parameters. This would indicate that the approach is physically correct.

From the material science point of view referred to in [3], it is known that the proposed approach cannot reproduce the physical process exactly. So different approximation methods can be expected to result in different sets of parameters and to show different approximation qualities. The goal of this contribution is to test if a good approximation can be found with low effort. The calculation of phase concentrations and resulting yield strength was done with a one-element-test. The resulting Yield strength for three different (but equally simple) procedures with ***MAT_254** and the reference from figure (2) is shown in figure (3). It can be seen, that the general hardening behavior can be reproduced well with the use of ***MAT_254** with a very simple three phase model.

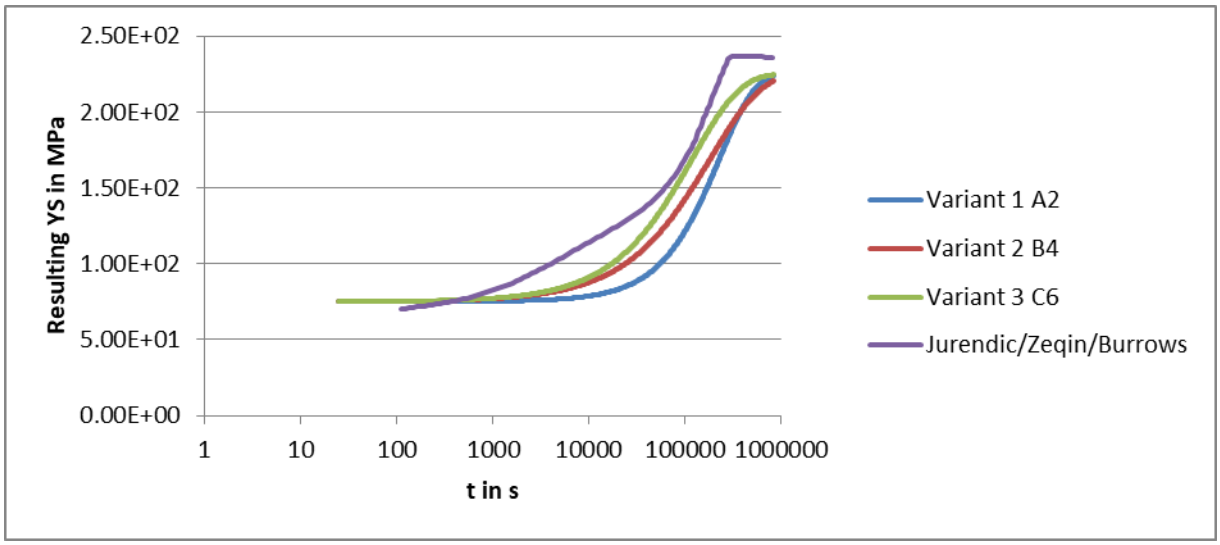

*Fig.5: Comparison of the resulting yield strength of 3 different procedures leading to different parameter sets for ***MAT_254** and the reference from [3]*

5 Discussion and further extension

From the data and theory in [3] it's clear that the real hardening effects of the precipitation are a combination of several mechanisms and several kinds of precipitation, which are simplified to a single mechanism here. From that it is fully clear, that the presented approach with only three distinct phases cannot fully reproduce the input data.

In [3] there was also a non-transient temperature load assumed. For a real process like paint bake, the temperature field is non-homogeneous and transient. In general, material model **MAT_254** is well-suited also for these kind of processes, but the calibration process required more data beside the results for 185°C.

As stated in [3], also the pre-strain of a structure has an influence on the paint bake behavior. For other cases it is also observed that a higher dislocation density speed up phase transformations in general. The dislocation density could be translated to the finite element world as equivalent plastic strain as both are the result of cold working. This leads to the extension of equation (2) with $\tau(T, eps) = \alpha(eps)\tau(T)$. Here, the kinetic accelerator $\alpha(eps)$ is a function of the plastic strain and can be given as user input.

Finally, to be able to take annealing effects into account, it is now possible in ***MAT_254** to describe the reduction of the equivalent plastic strain with a JMAK-type evolution equation:

$$\varepsilon_p = \varepsilon_p^{\text{start}} \left(1 - \left(1 - \alpha_{eq}(T)\right) \left(1 - e^{-\left(\frac{t}{\tau(T)}\right)^{n(T)}} \right) \right) \tag{6}$$

6 Summary

A first approach to describe the 'bake hardening' effect of an EN AW 6xxx lightweight aluminium alloy with ***MAT_254** was presented. It reproduces the general tendency very well, although it was based only on very limited data basis. With further available material data, the approach can easily be extended and it can be expected that the resulting representation of internal processes in aluminium alloys would be significantly enhanced. With a well-defined material card, it should be possible to simulate a process chain with a forming and the subsequent paint bake and, thus, the final property distribution in a component.

7 Literature

[1] Klöppel, T.: "The Structural Conjugate Heat Transfer Solver - Recent Developments", 11. European LS-Dyna Conference 2017, Salzburg

[2] Deschamps A, Brechet Y.: "Influence of predeformation and ageing of an Al–Zn–Mg alloy—II. Modeling of precipitation kinetics and yield stress", Acta Materialia, 1998;47:293-305

[3] Jurendic et al: "FE Implementation of AA6xxx Series Aluminium Pre-Strain Dependent Strengthening Response During Paint Bake", 11. European LS-Dyna Conference 2017, Salzburg